Alternatively Activated Macrophages Determine the Repair of the Infarcted Adult Murine Heart *(Shiraishi et al.)*

List of Supplemental Materials

- Supplemental Methods
- Supplemental Figure 1. Cardiac $CD206^+$ cells expressed macrophage markers.
- Supplemental Figure 2. The numbers of $CD68^+$ cells and $CD11c^+$ cells were increased post-MI in the area- and time-specific manners (Supplemental images to Figure 2C).
- Supplemental Figure 3. The majority of cardiac $CD11c^+$ cells presented a phenotype of M1-like pro-inflammatory macrophages and monocytes.
- Supplemental Figure 4. CD11c was expressed in $CD206^-$ cardiac cells but not in $CD206^+$ cardiac M2-like macrophages.
- Supplemental Figure 5. Collagen deposition, cardiac fibroblasts, and capillary formation in the myocardium of *Trib1*$^{-/-}$ mice were similar to those of WT littermates.
- Supplemental Figure 6. Local cell-proliferation occurred in cardiac M2-like macrophages of *Trib1*$^{-/-}$ mice and wild-type littermates.
- Supplemental Figure 7. Post-MI spatiotemporal changes of $CD11c^+$ cells in *Trib1*$^{-/-}$ mice were identical to those of WT littermates.
- Supplemental Figure 8. The transplanted BMDMs showed a similar phenotype to that of cardiac M2-like macrophages (Supplemental to Figure 4D).
- Supplemental Figure 9. Post-MI activation of cardiac fibroblasts was impaired in *Trib1*$^{-/-}$ mice.

- Supplemental 10. Post-MI collagen fiber formation in the infarcted myocardium was critically impaired in the *Trib1*$^{-/-}$ mouse heart (Supplemental data to Figure 6C).
- Supplemental Figure 11. Local cell-proliferation of cardiac M2-like macrophages was amplified by IL-4 treatment.
- Supplemental Figure 12. IL-4 treatment augmented the post-MI accumulation of cardiac fibroblasts solely in the infarcted myocardium (Supplemental to Figure 11A).
- Supplemental Figure 13. IL-4 treatment improved the capillary formation post-MI.
- Supplemental Figure 14. IL-4 treatment did not activate cardiac fibroblasts in vitro.
- Supplemental Figure 15. IL-4 treatment did not affect cardiac fibroblasts or capillary vessels in the intact (no MI) heart.
- Supplemental Figure 16. Supplemental data to Figure 13 (IL-1α and Osteopontin).
- Supplemental Figure 17. Most of cardiac M2-like macrophages disappeared at Day 1 post-MI.
- Supplemental Figure 18. Supplemental information regarding transplantation of bone marrow-derived macrophages (BMDMs).
- Supplemental Table 1. Echocardiographic data in *Trib1*$^{-/-}$ mice.
- Supplemental Table 2. Echocardiographic data in the IL-4 treatment study.
- Supplemental Table 3. Catheterization data in the IL-4 treatment study (Day 28 post-MI).

Supplemental Methods

Cardiac function measurement. Transthoracic echocardiography was performed by using a Vevo-770 (VisualSonics) with a 30 MHz high-frequency transducer under 1.0% isoflurane inhalation as previously described *(40,43)*. Left ventricular (LV) ejection fraction was calculated with the Simpson's method from the 2-dimensional tracing. LV end-diastolic and end-systolic dimensions were measured with the M-mode. LV end-diastolic and end-systolic areas were measured with the B-mode. Data were collected from 3 different measurements in a blinded manner. In addition, hemodynamic parameters were measured by using cardiac catheterization as previously described *(40,43)*. Briefly, under general anesthesia using isoflurane and mechanical ventilation, a catheter (SPR-839NR; Millar Instruments) was inserted into the LV cavity through the LV free wall. Intra-LV pressure signals were measured (MPVS-300; Millar Instruments) and digitally recorded with a data acquisition system (PowerLab 8/30; ADInstruments). The data were collected from at least 5 different measurements in a blinded manner.

RNA extraction and real-time PCR. Total RNA was extracted from cells or the heart tissue using the Gene Jet PCR purification Kit (Thermo Scientific) and quantified with a Nano-Drop 8000 spectrophotometer (Thermo Scientific). cDNA was synthesized by using the high-capacity cDNA Reverse Transcription Kit (Applied Biosystems) from 25 ng and 150 ng of total RNAs from M2-macrophages and the heart tissues, respectively. Real time PCR was performed by a Rotor-Gene 6000 (Qiagen) with a SYBR Green I master mix (Roche) in following conditions: 95°C for 10 minutes followed by 50 cycles at 95°C for 15 seconds, 64°C for 30 seconds and 72°C for 30 seconds. Gene expression levels were normalized by *Hprt*. The primers used are:

Il10	forward	5’- CGCTGTCATCGATTTCTCC -3’
	reverse	5’- ACACCTTGGTCTTGGAGCTT -3’
Vegfa	forward	5’- GTACCTCCACCATGCCAAGT -3’
	reverse	5’- GCATTCACATCTGCTGTGCT -3’
Spp1	forward	5’- GAGGAAACCAGCCAAGGTAA -3’
	reverse	5’- TAGTCCCTCAGAATTCAGCCA -3’
Il1a	forward	5’- CCATGATCTGGAAGAGACCA -3’
	reverse	5’- GACAAACTTCTGCCTGACGA -3’
Il1rn	forward	5’- ATGGAAATCTGCAGGGGACC -3’
	reverse	5’- CCCAGATTCTGAAGGCTTGC -3’
Col1a1	forward	5’- TGAGCCAGCAGATTGAGAAC -3’
	reverse	5’- CCAGTACTCTCCGCTCTTCC -3’
Col3a1	forward	5’- AGTCTGGAGTCGGAGGAATG -3’
	reverse	5’- AGGATGTCCAGAGGAACCAG -3
Mrc1 *(CD206)*	forward	5’- TGATTACGAGCAGTGGAAGC -3’
	reverse	5’- GTTCACCGTAAGCCCAATTT -3’
Retnla	forward	5’- AGGAACTTCTTGCCAATCCA -3’
	reverse	5’- ACAAGCACACCCAGTAGCAG -3’
Chil3	forward	5’- TGGTGAAGGAAATGCGTAAA -3’
	reverse	5’- GTCAATGATTCCTGCTCCTG -3’
Hprt	forward	5’- AGCGATGATGAACCAGGTTA -3’
	reverse	5’- GTTGAGAGATCATCTCCACC -3’

Microarray analysis. Total RNA of $CD206^{+}F4/80^{+}CD11b^{+}$ M2-like macrophages were isolated by FACS (see above) from the heart and the peritoneal cavity, amplified with the RNA Amplification System (NuGEN), and subjected to an Illumina's beads array platform with a Mouse WG-6 v2.0 Expression BeadChip (Illumina). Two independent biological replicates were prepared for each group category. The median per chip normalization was performed in each array. We analyzed only genes whose signal intensity was above the value of 90 in one of the biological duplicates. A two-fold change cut-off was used in order to identify differential lay expressed genes.

Immunohistochemistry. Immediately after cervical dislocation, the aorta of the mouse was clamped and ice-cold PBS was injected into the left ventricular cavity. The mouse heart was then perfused with ice-cold 4% of paraformaldehyde in PBS. The heart was removed, cut and embedded in O.C.T. compound (VWR International) and frozen in isopentane chilled in liquid nitrogen. The frozen tissue sections (8 μm thick) were incubated in PBS containing 0.1% of Triton X (Sigma-Aldrich) for 5 minutes at the room temperature, and the non-specific antibody-binding sites were pre-blocked with the blocking buffer (PBS plus 5% of goat serum or 5% of bovine serum albumin). Then, the primary antibodies were applied overnight at 4°C. After rinsing 3 times for 15 minutes in PBS, the sections were next incubated with appropriate fluorophore-conjugated secondary antibodies and 4',6-diamidino-2-phenylindole (DAPI) in the blocking buffer for 1 hour at the room temperature. Stained sections were mounted with a DAKO Fluorescence Mounting Medium and the digital images were acquired with an All-in-One microscope (Keyence, UK). The primary and secondary antibodies used in this study are as follows;

Primary antibody	Host	Dilution	Company Catalogue No.
anti-CD68	Rat	1:100	AbD Serotec MAC1957
AlexaFluor488-conjugated anti-CD206	Rat	1:100	BioLegend 141709
anti-CD11c	Hamster	1:100	AbD Serotec MCA1369
anti-CD90 (Thy1)	Rat	1:100	eBioscience 14-0901
anti-αSMA	Rabbit	1:100	Abcam ab5694
anti-Ki67	Rat	1:100	eBioscience 14-5698
anti-Cleaved caspase-3	Rabbit	1:200	Cell Signaling 9661
biotinylated Griffonia simplicifolia lectin I-isolectin B4	-	1:100	Vector L-1104

Secondary antibody	Host	Dilution	Company Catalogue No.
AlexaFluor 488-conjugated antibody	Goat	1:300	Invitrogen A11006

AlexaFluor 488-conjugated antibody	Donkey	1:300	Invitrogen A-21208
AlexaFluor 594-conjugated antibody	Goat	1:300	Invitrogen A-11007

Picrosirius red staining. The 8-μm frozen sections were incubated in 1.5% of phosphomolybic acid for 60 minutes, next in 0.1% of Picrosirius red for 15 minutes, and then in 0.5% of acetic acid solution for 3 minutes. After dehydration through increasing concentrations of ethanol to xylene, the sections were mounted using the DPX mounting medium (VWR International). The infarct size (the ratio of scar length to total left ventricular circumference) and the wall thickness were measured at five independent regions in the infarct area as previously described *(40).* The quantity of the collagen fraction was calculated by using a National Institute of Health image-analysis software (ImageJ). The infarct area was defined as the area in which >90% of cardiomyocytes were lost, and the border area was defined as adjacent to the infarct area with >50% of cardiomyocytes being alive.

Immunocytochemistry. The cells were fixed by 4% of paraformaldehyde in PBS for 5 minutes at room temperature. Except for the surface antigen staining, the cells were incubated in PBS containing 0.1% of Triton x100 for 5 minutes at the room temperature. Non-specific antibody binding sites were pre-blocked with PBS containing 5% of goat serum for 30 minutes at the room temperature. Then primary antibodies were applied onto the cells for 1 hour at room temperature. The primary antibodies used are: anti-vimentin (1:100, Abcam, ab24525), anti-αSMA (1:00, Abcam, ab5694), anti-CD68 (1:00, AbD Serotec, MCA1957), anti-CD14 (1:20,

PE-conjugated, eBioscience, 12-0141), and anti-F4/80 (1:20, PE-conjugated, eBioscience, 12-4801). After rinsing, cells were incubated with the fluorophore-conjugated secondary antibodies (1:300, AlexaFluor 488-conjugated or AlexaFluor 594-conjugated polyclonal, Invitrogen A11039, A-21208, or A-11037) and DAPI in blocking buffer for 1 hour at room temperature. The images were acquired using an All-in-One microscope (Keyence). The secondary antibodies used are as described for immunohistochemistry (above).

Supplemental Figure 1

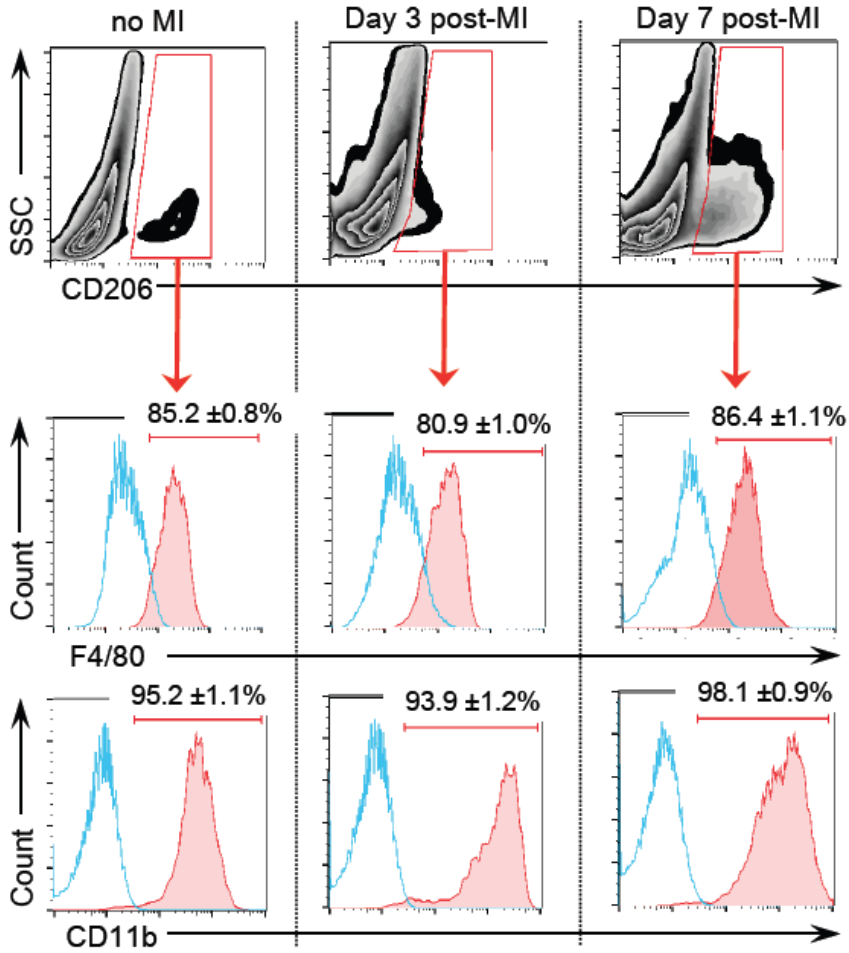

Supplemental Figure 1. Cardiac CD206^{+} cells expressed macrophage markers.
The flow cytometric analysis demonstrated that the CD206^{+} cell population in the intact (no MI) heart and Day 3 and Day 7 post-MI mouse heart was mostly positive for F4/80 and/or CD11b (shown in red), suggesting that the majority of CD206^{+} cells in the heart were macrophages/monocytes. The representative plots and the histograms from n=6 different hearts for each group are presented. The light blue lines indicate the IgG control data.

Supplemental Figure 2

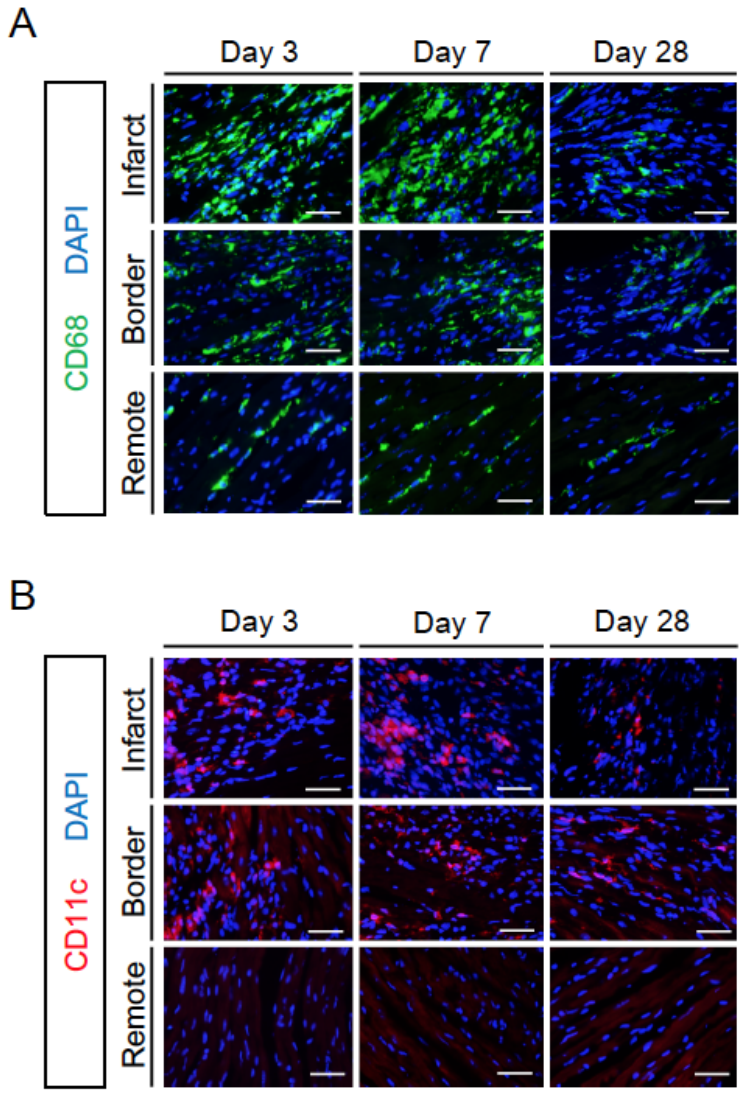

Supplemental Figure 2. The numbers of CD68$^+$ cells and CD11c$^+$ cells were increased post-MI in the area- and time-specific manners (Supplemental images to Figure 2C).
Immunohistochemistry demonstrated that CD68$^+$ cells (**a**; pan-macrophages) and CD11c$^+$ cells (**b**; mostly M1-like macrophages or monocytes) were increased in number in the infarct and border areas post-MI (from n=6 different hearts). The nuclei were stained with DAPI. Scale bars=50 μm. The numbers of these cells in each area at each time point were counted, averaged, and shown as graphs in Figure 2C. For images of CD68$^+$ cells in the intact (no MI) heart, see Figure 2A. CD11c$^+$ cell was rarely detected in the intact heart.

Supplemental Figure 3

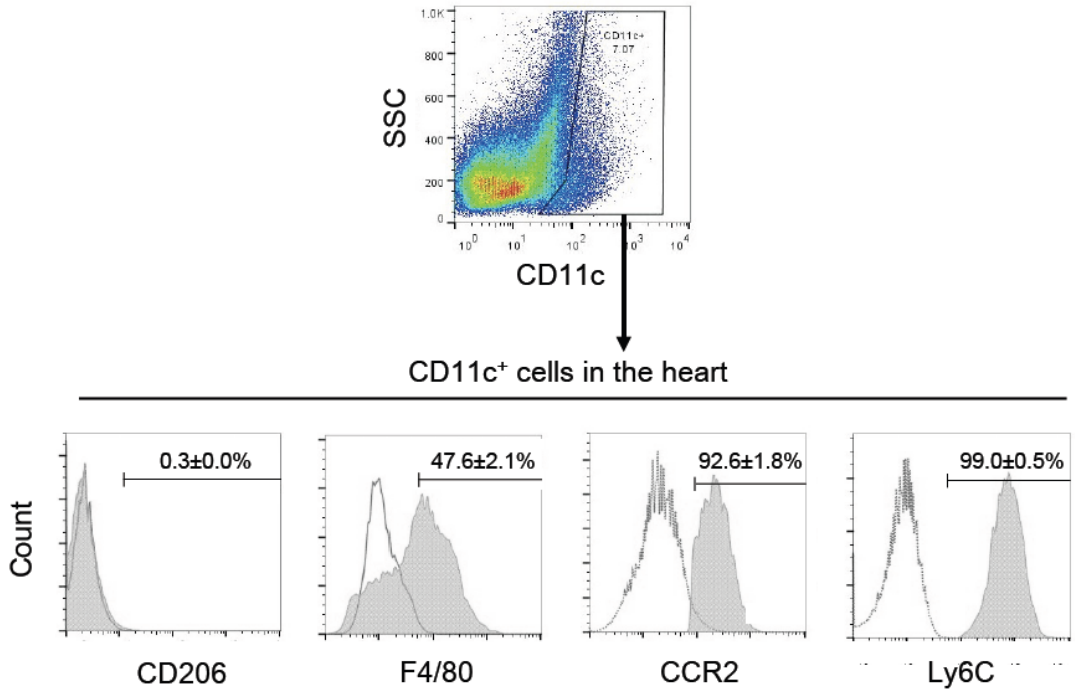

Supplemental Figure 3. The majority of cardiac CD11c$^+$ cells presented a phenotype of M1-like inflammatory macrophages and monocytes.

The flow cytometric analysis demonstrated that CD11c$^+$ cells from the MI mouse hearts (Day 7 post-MI) were negative for CD206 but positive for CCR2 and Ly6C (the shaded histogram). The open histograms indicate the IgG control data. The number of CD11c$^+$ cells in the normal (no MI) hearts was too small for the characterization. The representative histograms and the averaged values from n=6 different hearts are presented.

Supplemental Figure 4

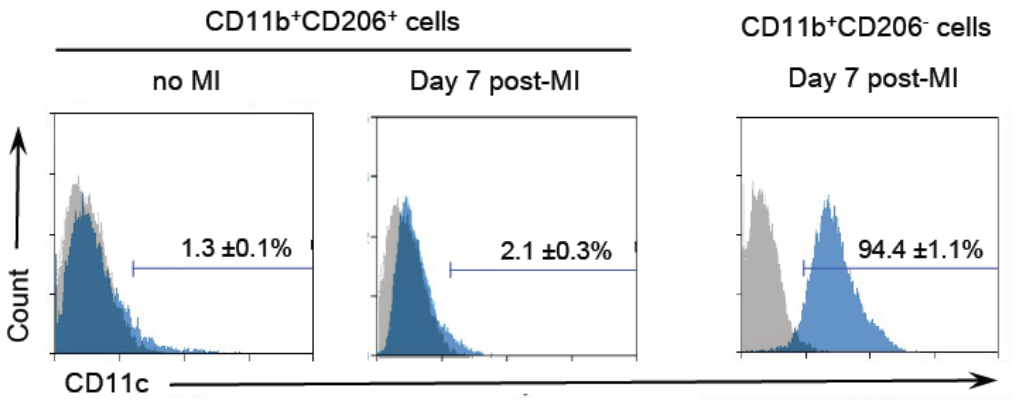

Supplemental Figure 4. CD11c was expressed in CD11b^{+}CD206^{-} cardiac cells but not in CD11b^{+}CD206^{+} cardiac M2-like macrophages.

The flow cytometric analysis demonstrated that CD11b^{+}CD206^{+} M2-like macrophages from the healthy (no MI) mouse hearts as well as from the MI mouse hearts (Day 7 post-MI) were negative for CD11c, whereas the majority of CD11b^{+}CD206^{-} cells from the post-MI Day 7 hearts was positive for CD11c (blue histograms). The grey histograms indicate the IgG control data). The number of CD11b^{+}CD206^{-} cells in the normal (no MI) hearts was too small for the flow cytometric characterization. The representative histograms and the averaged values from n=6 different hearts for each group are presented.

Supplemental Figure 5

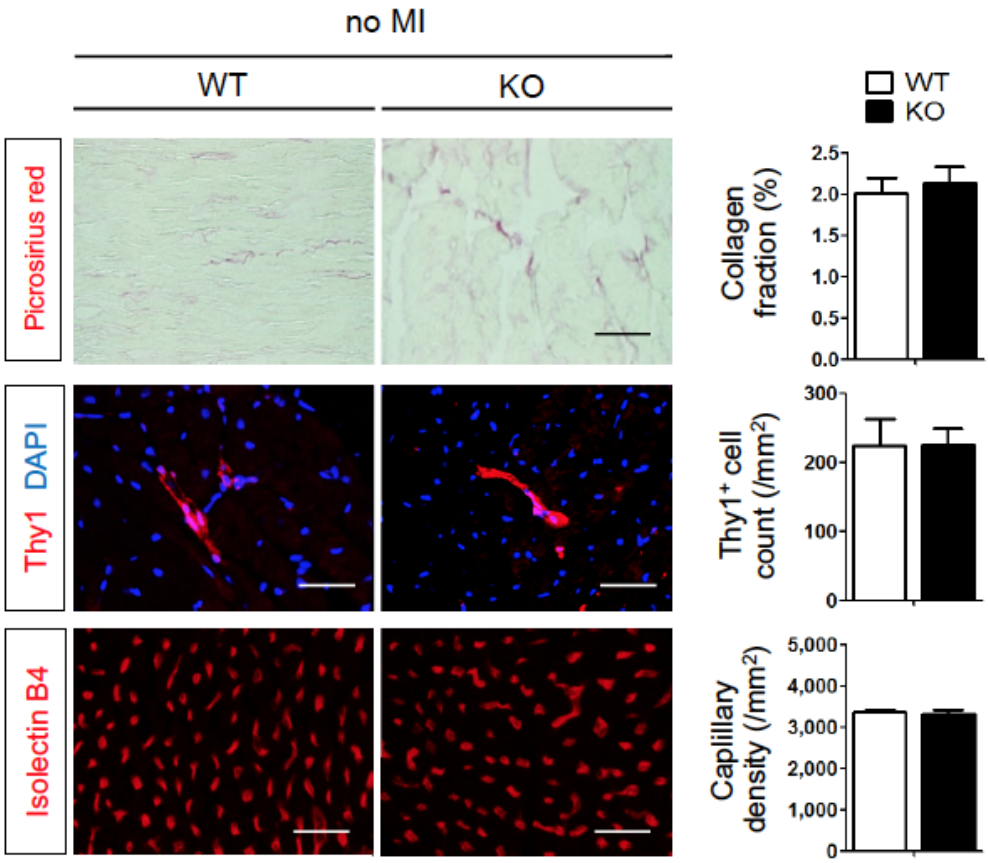

Supplemental Figure 5. Collagen deposition, cardiac fibroblasts, and capillary formation in the myocardium of Trib1$^{-/-}$ mice were similar to those of WT littermates.
The histological studies showed that the extracellular collagen deposition (picrosirius red staining), the frequency and distribution of cardiac fibroblasts (immunohistofluorescence for Thy1), and the capillary density (isolectin B4 staining) in intact (no MI) hearts were unchanged between the WT (wild-type littermates) and KO (*Trib1*$^{-/-}$ mice) groups. Scale bars=50 μm. The graphs show the averaged data from n=6 different hearts in each group; Student's t-test.

Supplemental Figure 6

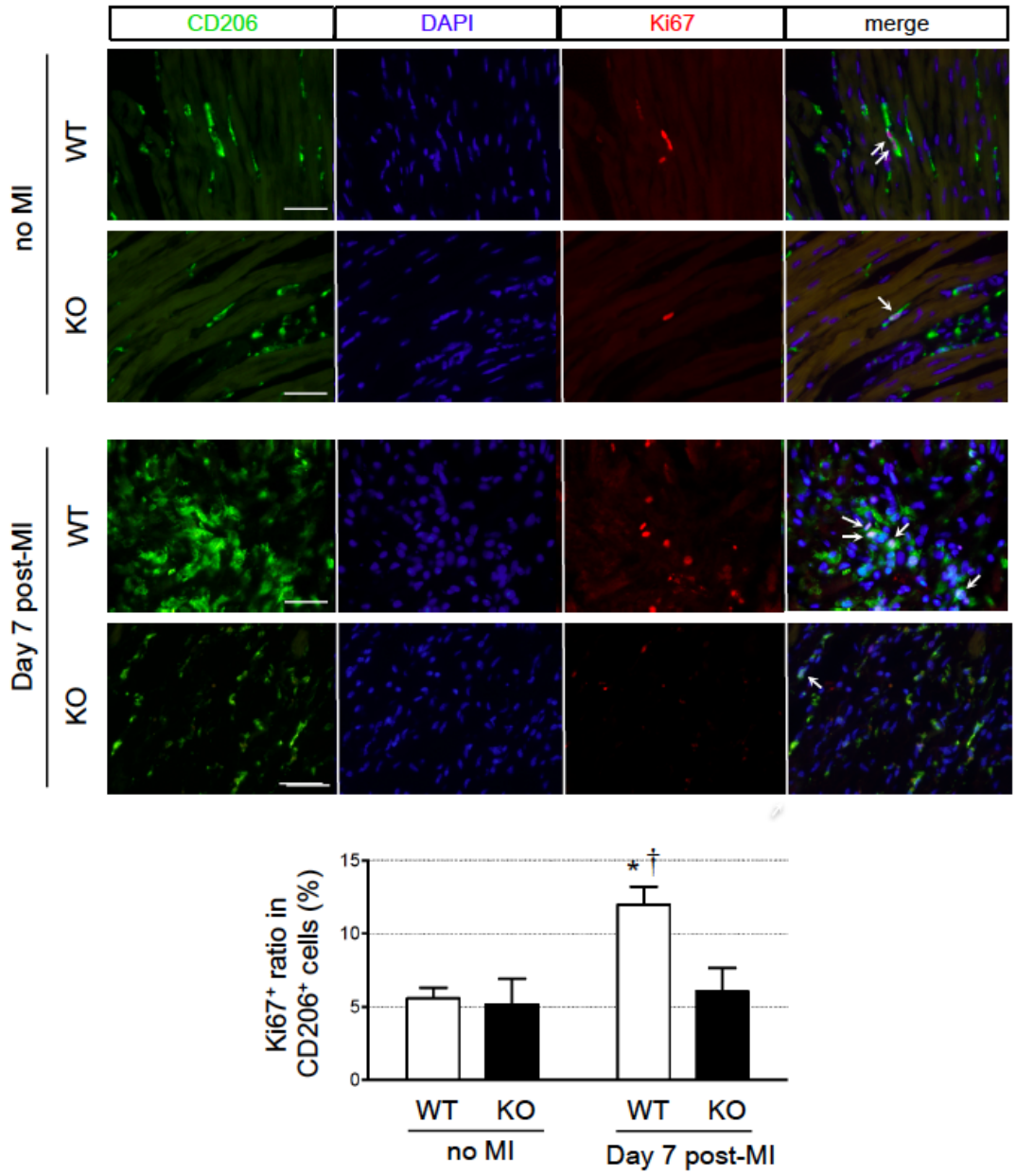

Supplemental Figure 6. Local cell-proliferation differently occurred in cardiac M2-like macrophages of Trib1$^{-/-}$ mice and wild-type littermates post-MI.
Immunohistochemistry demonstrated that CD206^{+} cardiac M2-like macrophages expressed Ki67, suggesting their local proliferation in the normal (no MI) hearts, at a similar ratio between WT (wild-type littermates) and KO (*Trib1*$^{-/-}$) mice. This ratio was increased post-MI in WT mice, but not in KO mice. n=6 different hearts. Scale bars=50 μm. **P*<0.05 *versus* the KO group at the same time point, †*P*<0.05 *versus* no MI value in each group; repeated measures ANOVA.

Supplemental Figure 7

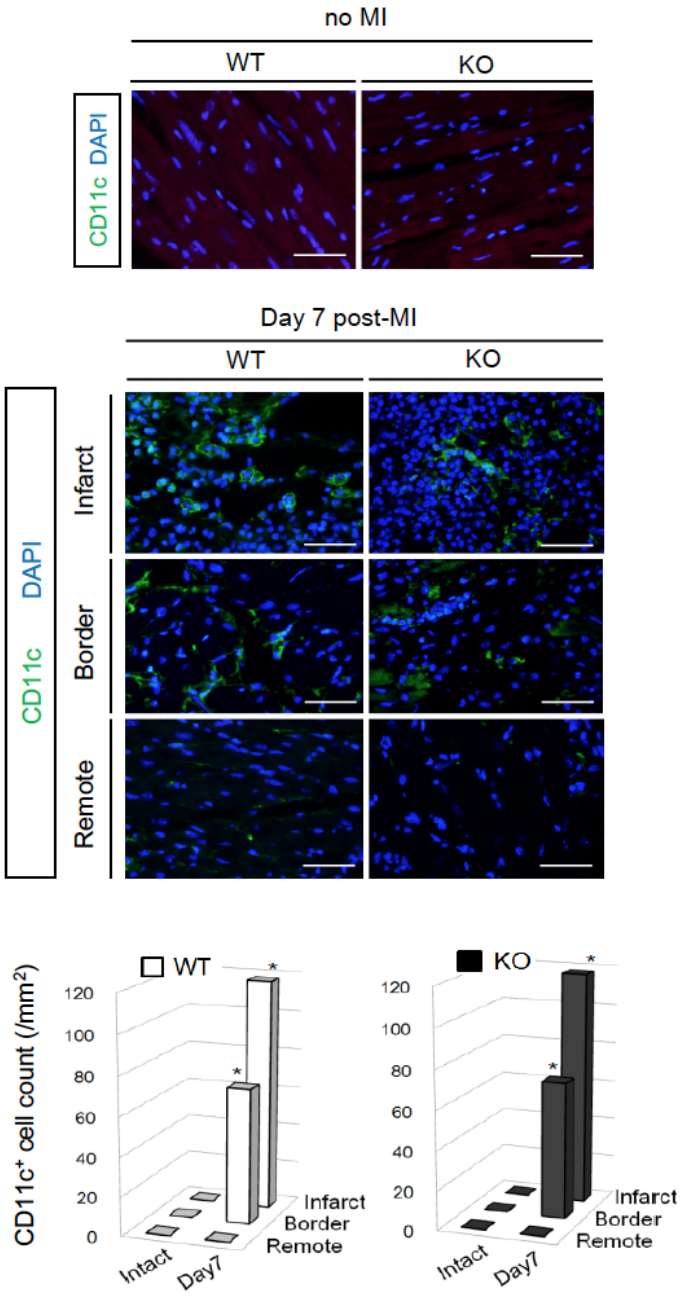

Supplemental Figure 7. Post-MI spatiotemporal changes of CD11c$^+$ cells in Trib1$^{-/-}$ mice were identical to those of WT littermates.
Immunohistochemistry demonstrated that pre- and post-MI dynamics of CD11c$^+$ cells (mostly pro-inflammatory macrophages/monocytes) was not changed in the KO group (*Trib1*$^{-/-}$ mice) compared to the WT group (wild-type littermates). Scale bars=50 μm. The graphs show the averaged CD11c$^+$ cell numbers in each area at each time post-MI, highlighting the similar dynamics of CD11c$^+$ cells between the two groups. n=5-6 at each point in each group, *P<0.05 *versus* the intact (no MI) heart in each group; repeated measures ANOVA.

Supplemental Figure 8

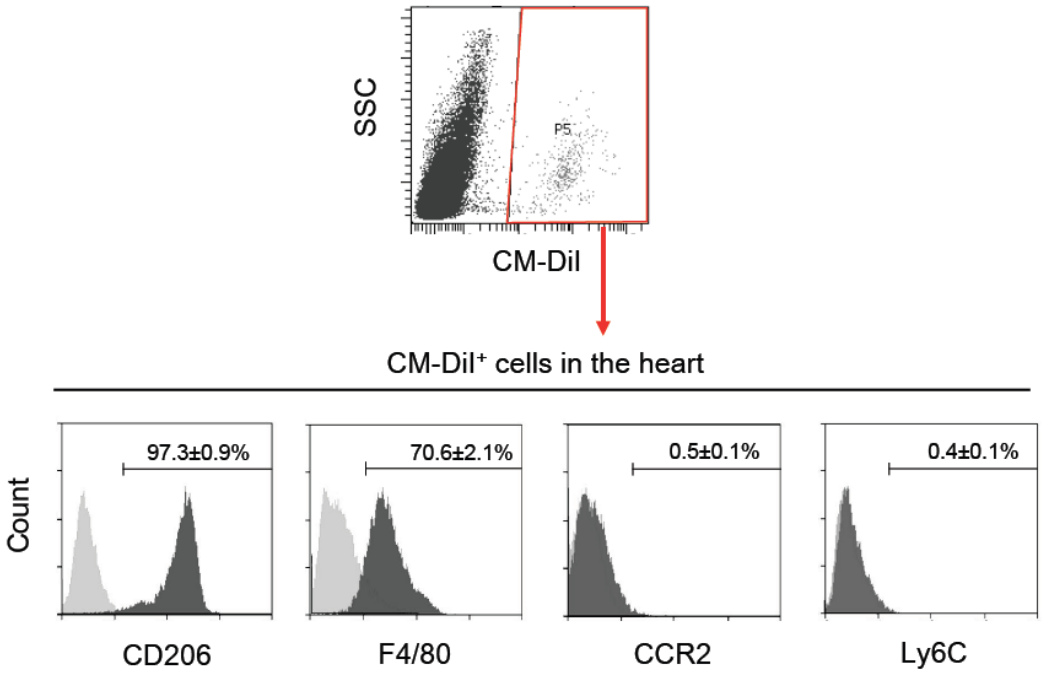

Supplemental Figure 8. The transplanted BMDMs showed a similar phenotype to that of cardiac M2-like macrophages (Supplemental to Figure 4D).

At Day 7 after intrapericardial transplantation of bone marrow-derived macrophages (BMDMs; labeled with CM-DiI) from WT mice into the KO (*Trib1*$^{-/-}$) mice with MI, the hearts were enzymatically digested. CM-DiI^{+} transplanted cells in the non-cardiomyocyte heart cell suspension were characterized by the flow cytometry for CD206, F4/80, CCR2, and Ly6C (dark-gray histograms). The light-gray histograms indicate the IgG control data. CM-DiI^{+} transplanted BMDMs showed the same expression pattern as cardiac M2-like macrophages in WT mice (refer to Figure 1A and 1B). The representative histograms and the averaged values from n=6 different hearts are presented.

Supplemental Figure 9

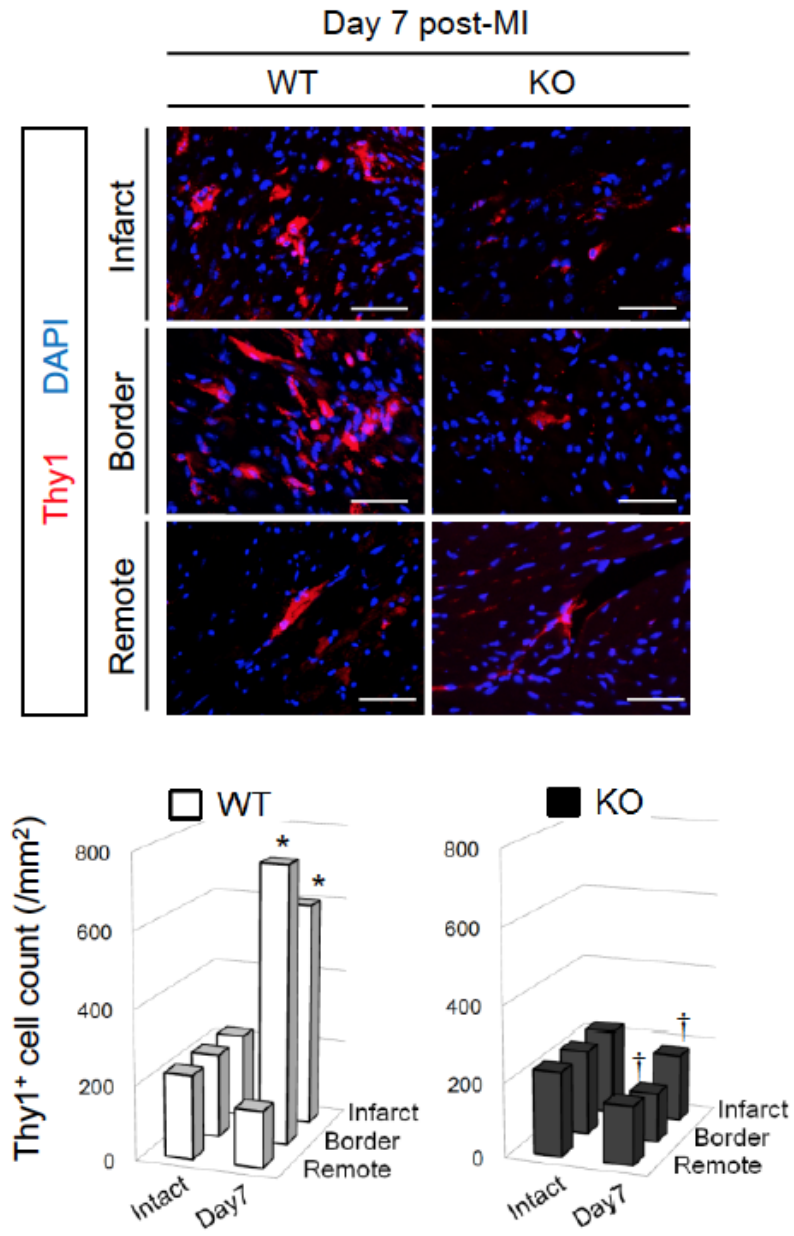

Supplemental Figure 9. Post-MI activation of cardiac fibroblasts was impaired in Trib1$^{-/-}$ mice. Immunohistochemistry demonstrated that the increase of Thy1^{+} fibroblasts in the infarct and border areas at Day 7 post-MI in the WT group (wild-type littermates) was entirely abolished in the KO group (*Trib1*$^{-/-}$ mice*)*. Fibroblast dynamics in the remote area was not affected in the KO group compared to the WT group. Scale bars=50 μm. See Supplemental Figure 5 for the images in the intact (no MI) hearts. n=6 and 5 in the WT and KO groups, respectively, **P*<0.05 *versus* the intact (no MI) heart in each group, †*P*<0.05 *versus* the WT group in the corresponding time and area; repeated measures ANOVA.

Supplemental Figure 10

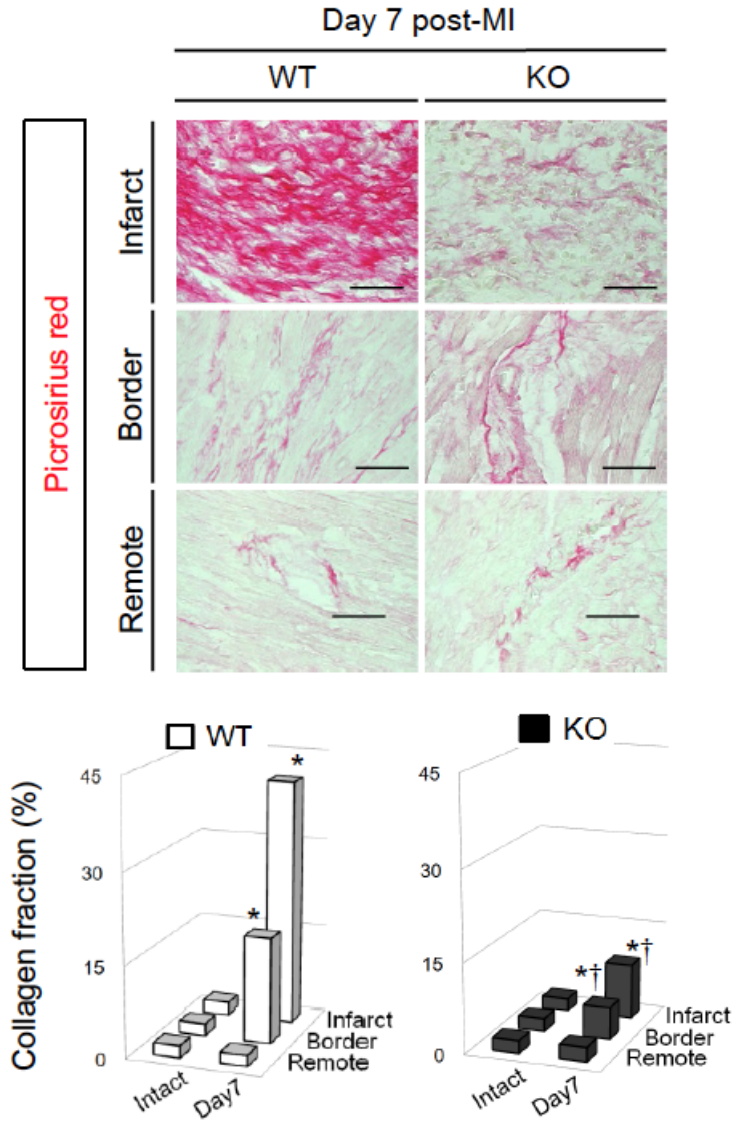

Supplemental Figure 10. Post-MI collagen fiber formation in the infarcted myocardium was critically impaired in the Trib1$^{-/-}$ mouse heart (Supplemental data to Figure 6C).
Picrosirius red staining demonstrated that the fibrotic connective tissue formation in the infarct and border areas at Day 7 post-MI hearts was largely attenuated in the KO group (*Trib1*$^{-/-}$ mice), compared to the WT group (wild-type littermates). The images for the infarct area are the same as Figure 6C. See Supplemental Figure 5 for the images of intact hearts. The graphs show the calculated collagen volume fraction in each area pre-MI (intact) and Day 7 post-MI. The collagen deposition in the remote area was similarly low in both the KO and WT groups. Scale bars=50 μm, n=6 and 5 different hearts in the WT and KO groups, respectively, **P*<0.05 *versus* the intact (no MI) heart in each group, †*P*<0.05 *versus* the WT group at the corresponding time and area; repeated measures ANOVA.

Supplemental Figure 11

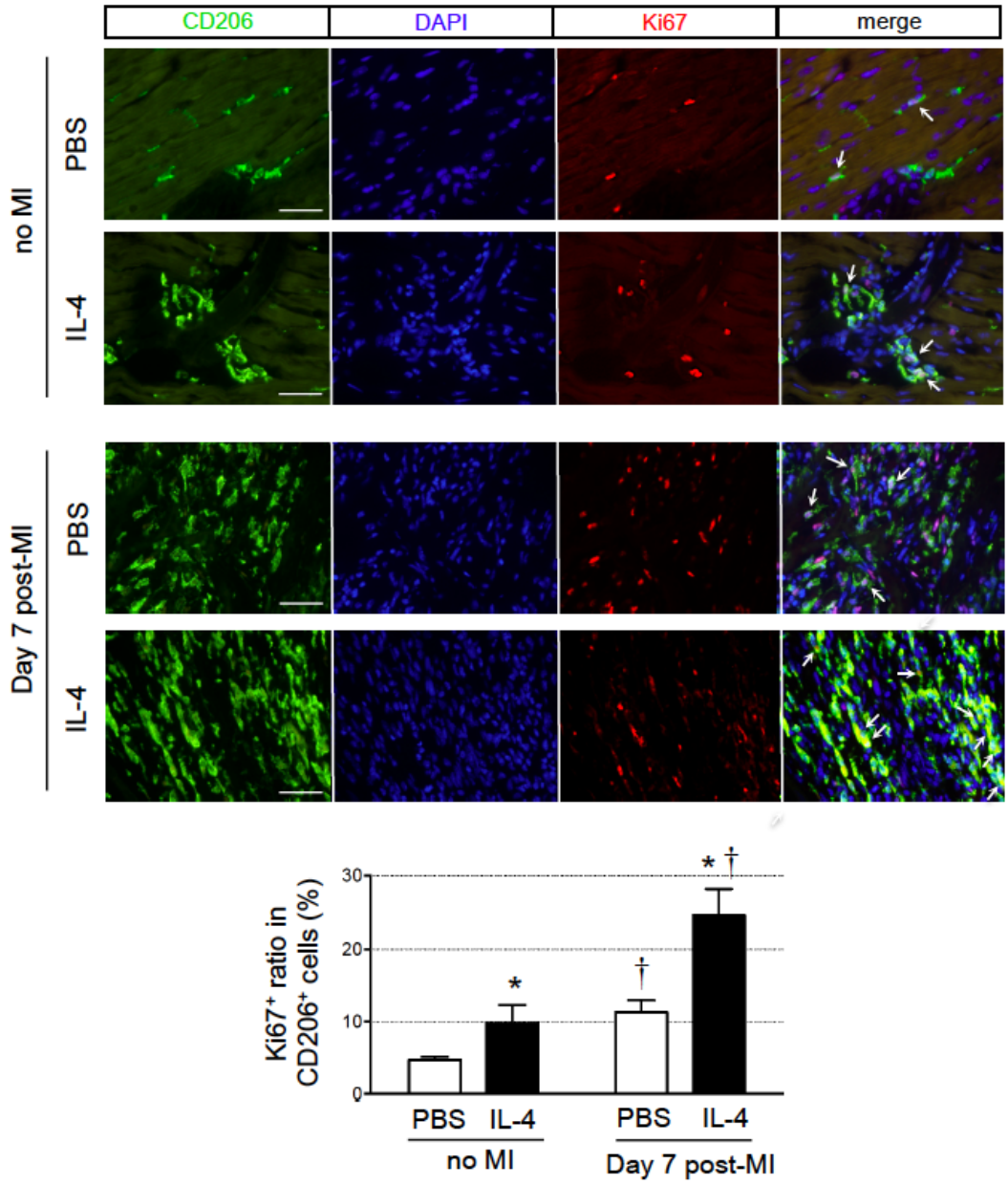

Supplemental Figure 11. Local cell-proliferation of cardiac M2-like macrophages was amplified by IL-4 treatment both before and after MI.

Immunohistochemistry demonstrated that the IL-4 group (IL-4 treatment) increased the Ki67 expression of $CD206^+$ cardiac M2-like macrophages in the no-MI heart, suggesting an increased local cell-proliferation of these cells, compared with the PBS group (PBS control injection). In addition, proliferation ($Ki67^+$ rate) of $CD206^+$ cardiac M2-like macrophages was increased following MI in both groups, and this increase was more extensive in the IL-4 group compared to the PBS group. n=6 different hearts. Scale bars=50 μm. *P<0.05 *versus* the PBS group of the same time point, $^{\dagger}P$<0.05 *versus* no MI value in each group; repeated measures ANOVA.

Supplemental Figure 12

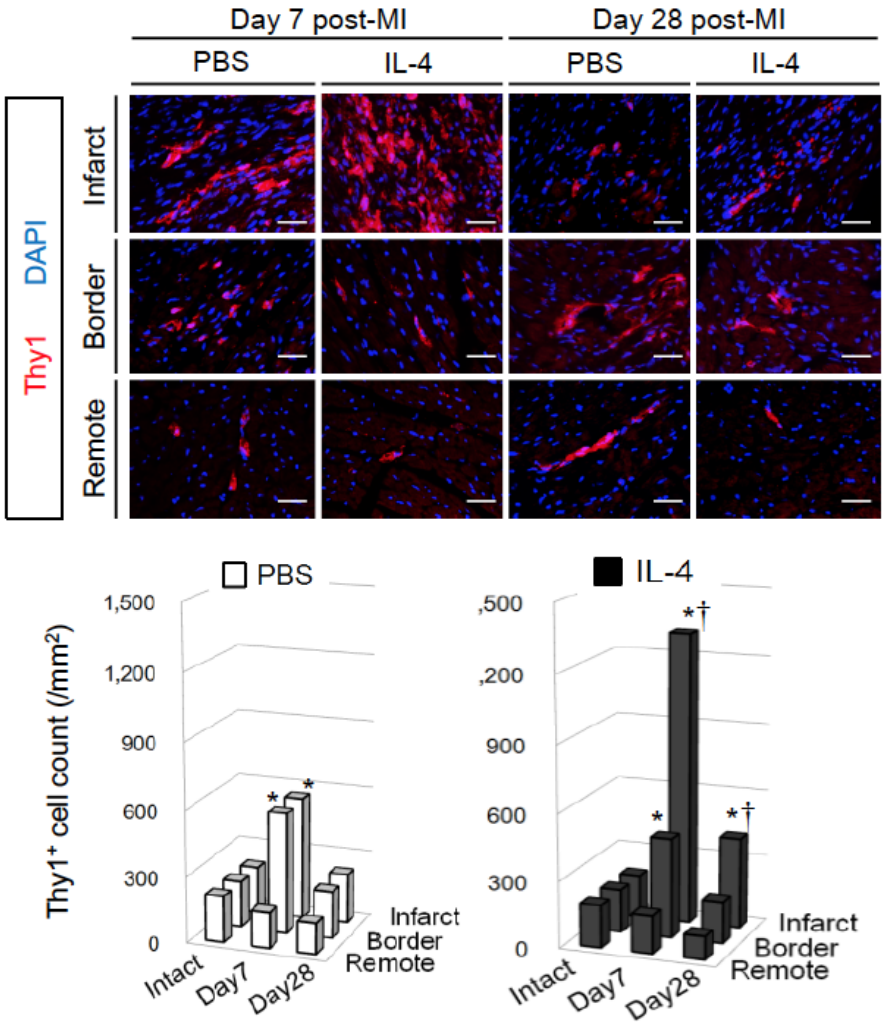

Supplemental Figure 12. IL-4 treatment increased the post-MI accumulation of cardiac fibroblasts solely in the infarcted area (Supplemental to Figure 11A).
Immunohistochemistry demonstrated that the accumulation of Thy1$^+$ cardiac fibroblasts in the infarct area at Day 7 and 28 post-MI was increased in the IL-4 group (IL-4 treatment) compared with the PBS group (PBS control injection). In contrast, the fibroblast dynamics in the border and remote areas was unchanged between the groups. Scale bars=50 μm. The graphs show the averaged Thy1$^+$ cell numbers in each area, highlighting the above findings. n=6 for each point in each group, **P*<0.05 *versus* intact (no MI) heart in each group, †*P*<0.05 *versus* the PBS group at the corresponding time and area; repeated measures ANOVA.

Supplemental Figure 13

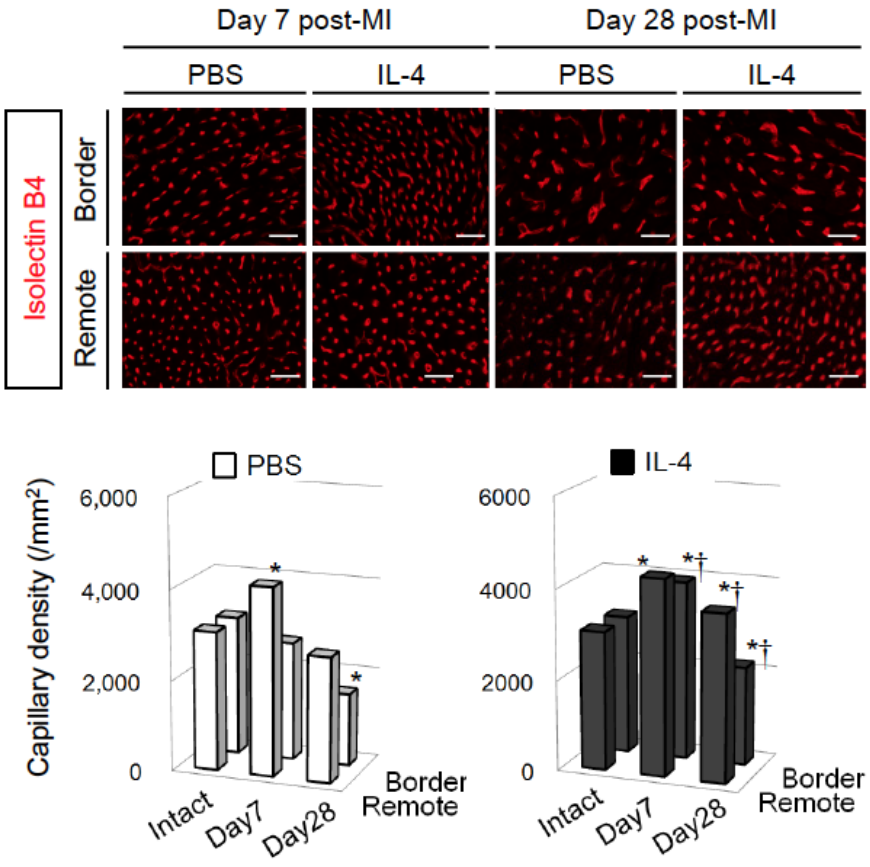

Supplemental Figure 13. IL-4 treatment improved the capillary formation post-MI.
Isolectin B4 staining demonstrated that the density of the capillary vessels was increased at Day 7 and 28 post-MI in the IL-4 group (IL-4 treatment) compared to the PBS group (PBS injection). The capillary density of the intact (no MI) hearts was not changed by IL-4 treatment (see Supplemental Figure 15 for the relevant images). The graphs indicate the averaged capillary density in each area at each point. Scale bars=50 μm. n=6 different hearts were studied at each point, **P*<0.05 *versus* the intact (no MI) heart in each group, †*P*<0.05 *versus* the PBS group at the corresponding time and area; repeated measures ANOVA.

Supplemental Figure 14

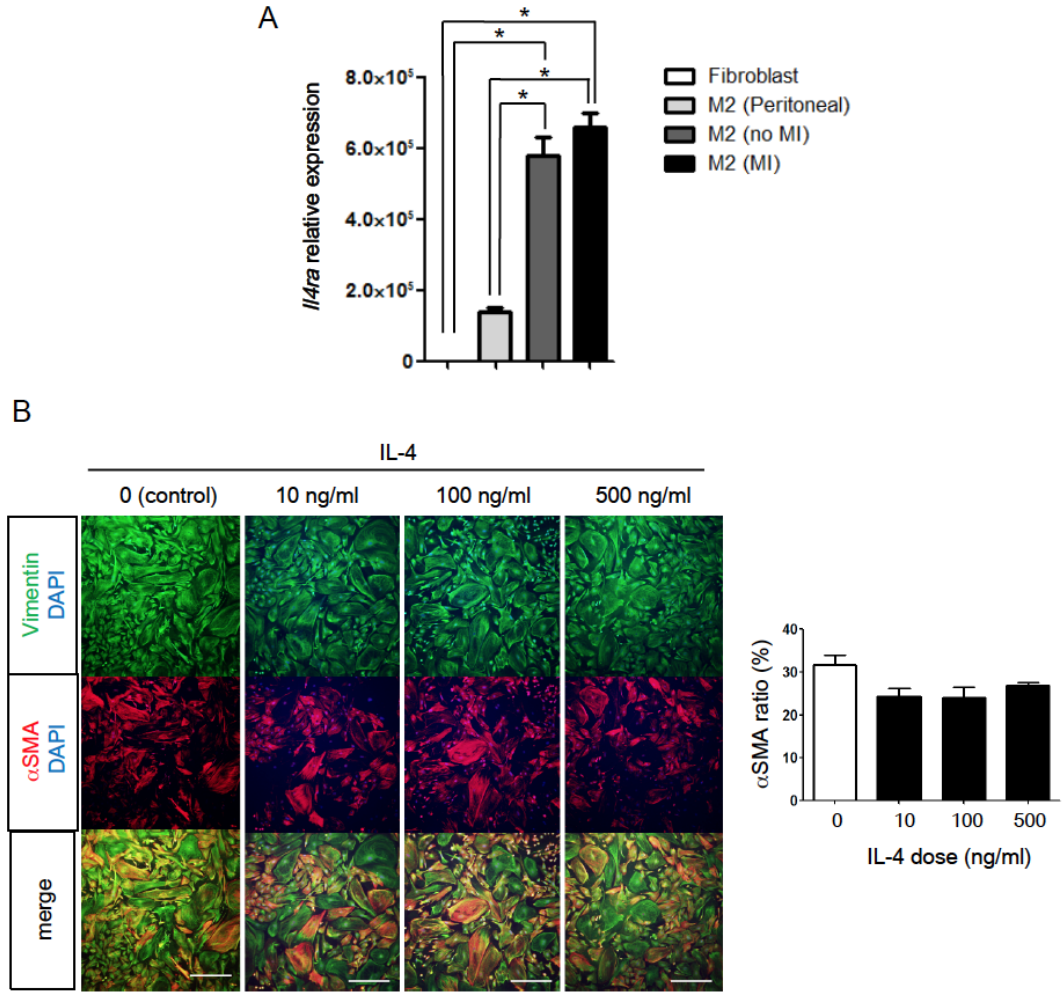

Supplemental Figure 14. IL-4 treatment did not activate cardiac fibroblasts in vitro.
(A) The quantitative RT-PCR analysis uncovered that the expression of *Il4ra (IL-4RA)* in primary cardiac fibroblasts (Fibroblast) was markedly lesser compared to that of M2-like macrophages from the intact heart [M2 (no MI)] and from the Day 7 post-MI heart [M2 (MI)]. The expression in M2-macrophages from the peritoneal cavity of the normal mice [M2 (Peritoneal)] is also shown for reference. The expression of *Il4ra* in fibroblasts is assigned to be 1.0 and the relative expression to this is presented. n=6 in each group, **P*<0.05; ANOVA.
(B) In vitro culture in the presence of recombinant IL-4 (10-500 ng/ml) for 48 hours did not increase the activation (transformation into αSMA^+ myofibroblasts) of primary cardiac fibroblasts. αSMA ratio = the ratio of $vimentin^+\alpha SMA^+$ myofibroblasts in $vimentin^+$ fibroblasts. Scale bars=200 μm, n=7 or 8 in each group; ANOVA.

Supplemental Figure 15

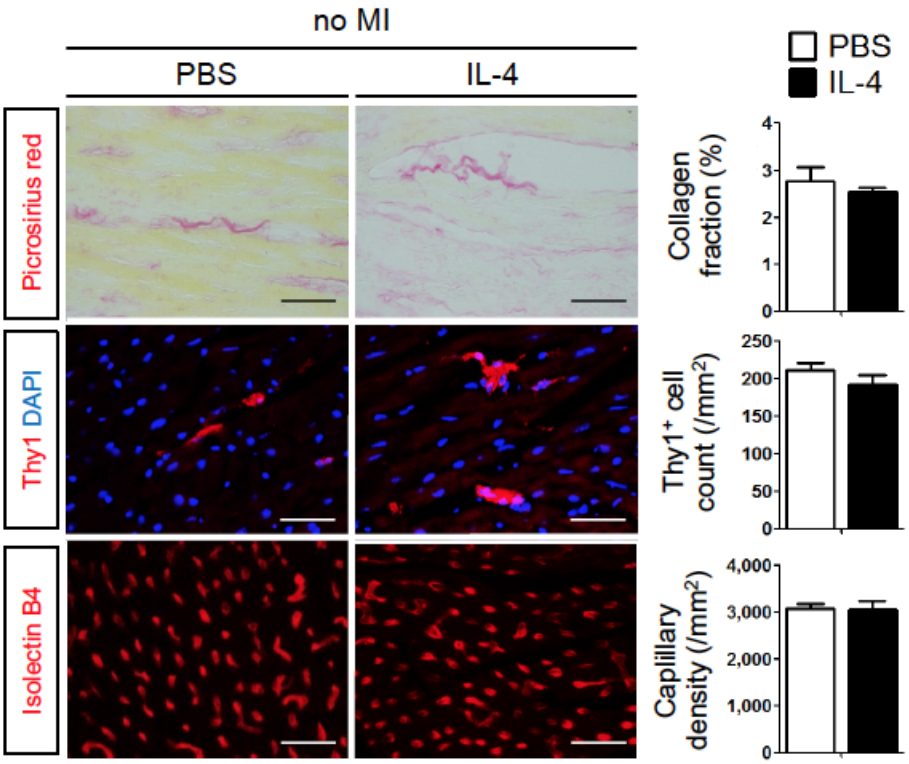

Supplemental Figure 15. IL-4 treatment did not affect cardiac fibroblasts or capillary vessels in the intact (no MI) heart.
The extracellular collagen deposition (picrosirius red staining), presence of cardiac fibroblasts (immunohistofluorescence for Thy1 with DAPI counter staining), and capillary vessels (isolectin B4 staining) were comparable between the PBS (PBS injection to the intact heart) and IL-4 (IL-4 treatment to the intact heart) groups. The graphs show the quantified data from the histological images. Scale bars=50 μm, n=6 different hearts for each group; Student's t-test.

Supplemental Figure 16

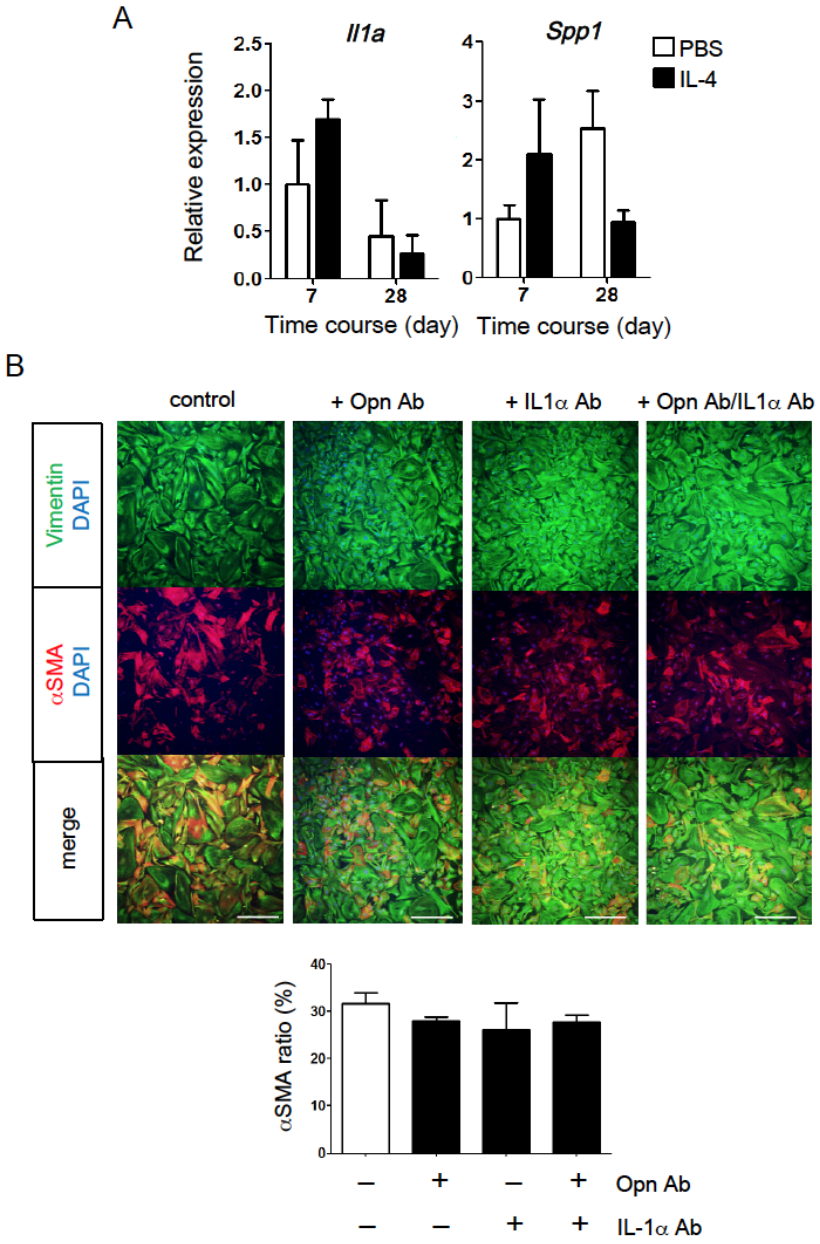

Supplemental Figure 16. Supplemental data to Figure 13 (IL-1α and Osteopontin).
(A) The quantitative RT-PCR analysis showed that the expression of *Il1a (IL-1α)* and *Spp1* (*osteopontin)* in the whole ventricle samples tended to be up-regulated (not statistically significant) at Day 7 post-MI in the IL-4 group, compared to the PBS group. n=6 for each point in each group; repeated measures ANOVA.
(B) Culture with neutralizing antibodies to osteopontin and/or IL-1α for 48 hours did not affect the activation of cardiac fibroblasts (transformation into αSMA^+ myofibroblasts). αSMA ratio = the ratio of $vimentin^+\alpha SMA^+$ myofibroblasts in $vimentin^+$ fibroblasts. Scale bars=200 μm, n=8 in each group; ANOVA.

Supplemental Figure 17

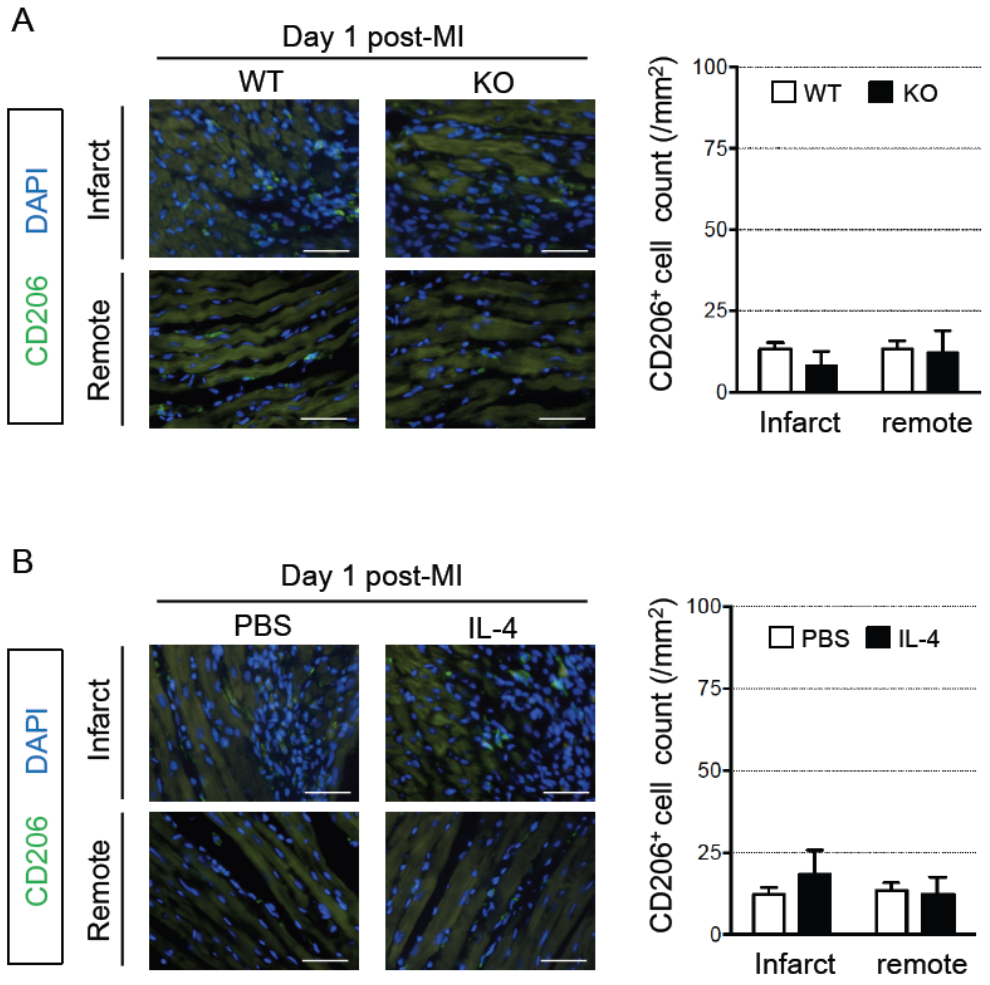

Supplemental Figure 17. Most of cardiac M2-like macrophages disappeared at Day 1 post-MI.
(A) Immunohistochemistry revealed that cardiac-resident cardiac $CD206^+$ cells in the normal hearts (refer to Figure 4A) predominantly disappeared at Day 1 post-MI in both the WT (wild-type littermate mice) and KO (*Trib1*$^{-/-}$ mice) groups. The nuclei were stained with DAPI. Scale bars=50 μm. n=6 different hearts.
(B) Similarly, only minimum numbers of $CD206^+$ cells were detected by immunohistostaining in the heart at Day 1 post-MI in both the PBS (control PBS treatment) and IL-4 (IL-4 treatment) groups. Please refer to Figure 7. Scale bars=50 μm. n=6 different hearts.

Supplemental Figure 18

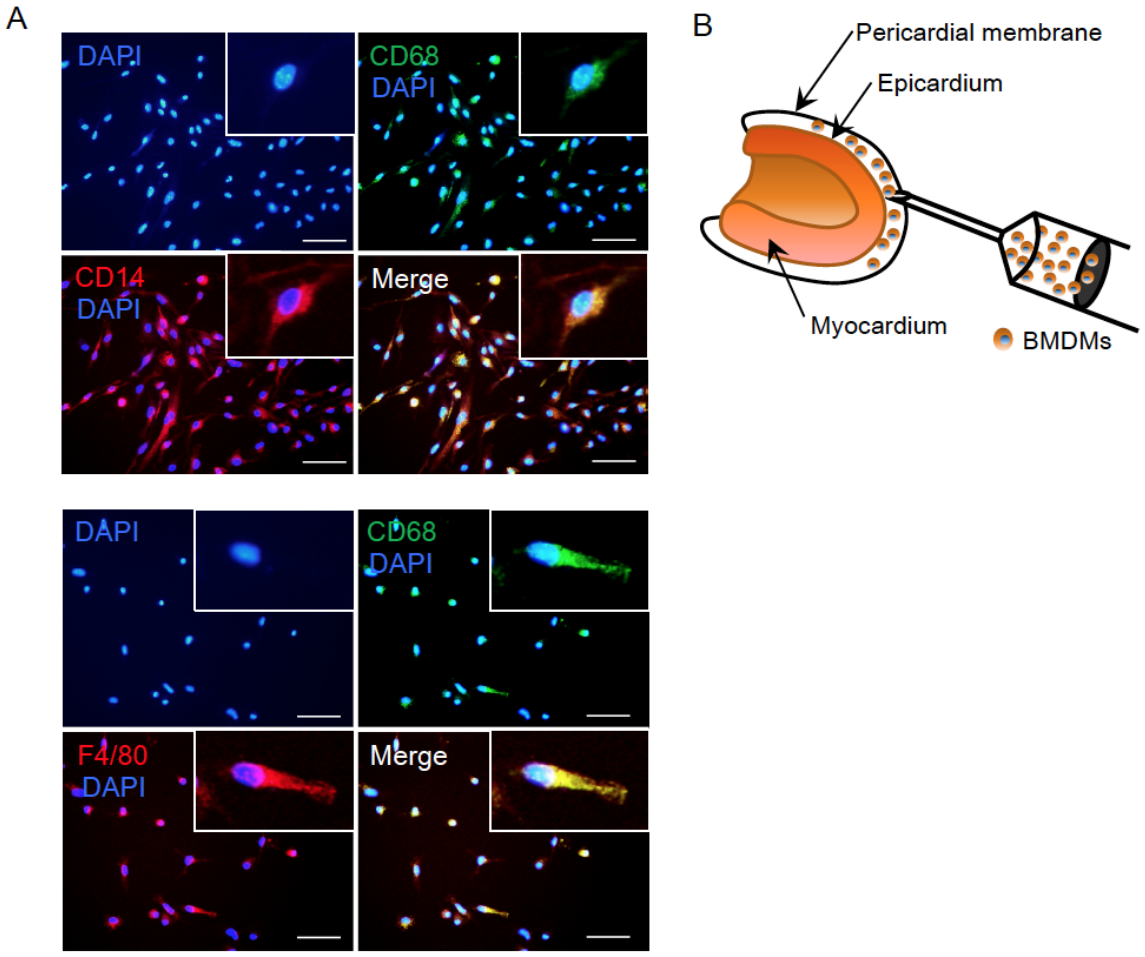

Supplemental Figure 18. Supplemental information regarding transplantation of bone marrow-derived macrophages (BMDMs).

(A) Immunocytochemistry demonstrated that the majority of BMDMs produced from WT mice were $CD14^{+}CD68^{+}$ and $F4/80^{+}CD68^{+}$, thus confirming that these cells were macrophages. The nuclei were stained with DAPI. Scale bars=100 μm.

(B) The scheme of BMDM transplantation is presented. The collected BMDMs were mixed with Matrigel and injected into the pericardial cavity using a needle-syringe under left thoracotomy with mechanical ventilation.

Supplemental Table 1

	LVDd (mm)			LVDs (mm)		
	Day 0	Day 7	Day 28	Day 0	Day 7	Day 28
WT	3.5±0.1	4.0±0.1	4.8±0.1	2.1±0.1	3.0±0.1*	4.0±0.1
KO	3.5±0.1	4.2±0.2	5.7	2.1±0.1	3.6±0.2	5.4
KO+BMDMs	3.6±0.1	4.0±0.1	4.6±0.1	2.2±0.1	3.1±0.1*	3.9±0.1
KO+IL-4	3.4±0.1	4.3±0.2	6.7	2.0±0.1	3.7±0.2	6.5

	LV diastolic endocardial area (mm^2)			LV systolic endocardial area (mm^2)		
	Day 0	Day 7	Day 28	Day 0	Day 7	Day 28
WT	10.9±0.2	14.8±0.4*	20.2±0.2	6.6±0.1	11.7±0.4*	17.2±0.4
KO	11.2±0.5	17.2±0.5	24.2	6.8±0.3	15.5±0.6	23.3
KO+BMDMs	11.6±0.6	14.5±0.3*	19.9±0.4	7.1±0.4	11.4±0.3*	16.9±0.3
KO+IL-4	10.5±0.2	17.9±1.4	29.1	6.4±0.1	16.2±1.4	26.6

	LVEF (%)			FAC (%)		
	Day 0	Day 7	Day 28	Day 0	Day 7	Day 28
WT	70.8±0.7	50.1±1.6*	32.9±1.2	39.5±0.4	21.5±0.9*	14.5±1.2
KO	70.9±0.6	29.1±1.4	9.4	39.4±0.3	10.0±1.0	3.7
KO+BMDMs	71.0±0.3	47.1±1.1*	33.4±0.5	39.4±0.3	21.1±1.1*	14.8±0.3
KO+IL-4	70.6±0.7	28.5±1.7	17.8	39.3±0.3	9.5±0.6	10.1

	FS (%)			HR (bpm)		
	Day 0	Day 7	Day 28	Day 0	Day 7	Day 28
WT	39.3±0.5	25.2±0.9*	15.6±0.7	548±9	542±7	544±10
KO	39.4±0.5	13.5±0.7	4.2	563±5	558±11	561.0
KO+BMDMs	39.6±0.3	23.3±0.7*	15.8±0.3	552±11	540±8	558±9
KO+IL-4	39.0±0.6	13.2±0.8	8.7	560±6	532±12	513.0

Supplemental Table 1. Echocardiographic data in Trib1$^{-/-}$ mice.
WT=wild-type littermate; KO=*Trib1*$^{-/-}$ mice; KO+BMDMs=*Trib1*$^{-/-}$ *mice* received intra-pericardial transplantation of BMDMs (bone marrow-derived macrophages); KO+IL-4=*Trib1*$^{-/-}$ mice received IL-4 treatment. Day 0=no MI; Day 7 and 28 =Day 7 and 28 post-MI. LVDd=left ventricular diastolic dimension; LVDs=left ventricular systolic dimension; LVEF=left ventricular ejection fraction; FAC=fractional area change; FS=fractional shortening; HR=heart rate. Sample number (Day 0, Day 7, Day 28) = (12, 10, 10) in the WT group, (12, 5, 1) in the KO group, (10, 6, 6) in the KO+BMDMs group, and (12, 3, 1) in the KO+IL-4 group, *P<0.05 *versus* the KO group at the corresponding time-point; repeated measures ANOVA (Day 28 data were not included in the calculation because n=1 in the KO and KO+IL-4 groups).

Supplemental Table 2

	LVDd (mm)			LVDs (mm)		
	Day 0	Day 7	Day 28	Day 0	Day 7	Day 28
PBS	3.5±0.2	3.8±0.1	4.5±0.1	2.1±0.1	2.9±0.1	3.6±0.1
IL-4	3.4±0.2	3.4±0.1*	4.0±0.1*	2.0±0.1	2.5±0.1*	2.9±0.1*

	LV diastolic endocardial area (mm^2)			LV systolic endocardial area (mm^2)		
	Day 0	Day 7	Day 28	Day 0	Day 7	Day 28
PBS	10.1±0.3	13.5±0.4	17.7±0.7	6.2±0.2	10.8±0.3	14.0±0.5
IL-4	10.3±0.3	10.6±0.3*	14.3±0.4*	6.1±0.7	8.1±0.2*	10.1±0.3*

	LVEF (%)			FAC (%)		
	Day 0	Day 7	Day 28	Day 0	Day 7	Day 28
PBS	72.1±0.5	48.9±1.6	42.2±1.3	39.0±0.8	20.1±0.9	20.4
IL-4	73.7±0.6	54.7±1.2*	52.4±0.5*	40.9±0.4	23.6±1.0*	26.2±0.9*

	FS (%)			HR (bpm)		
	Day 0	Day 7	Day 28	Day 0	Day 7	Day 28
PBS	40.4±0.5	24.3±0.9	20.7±0.7	540±16	541±10	536±9
IL-4	41.6±0.5	27.7±0.7*	26.5±0.3*	548±13	551±12	553±9

Supplemental Table 2. Echocardiographic data in the IL-4treatment study.
PBS group=injection of PBS; IL-4 group=IL-4 treatment; Day 0=no MI; Day 7 and 28 = Day 7 and 28 post-MI; LVDd=left ventricular diastolic dimension; LVDs=left ventricular systolic dimension; LVEF=left ventricular ejection fraction; FAC=fractional area change; FS=fractional shortening; HR=heart rate. n=12 for each point in each group, *P<0.05 *versus* the PBS group at the corresponding time-point; repeated measures ANOVA.

Supplemental Table 3

	Max Pressure (mmHg)	Min Pressure (mmHg)	Mean Pressure (mmHg)
PBS	107.7±2.8	15.3±0.7	50.9±1.6
IL4	121.6±1.1*	7.5±0.5*	62.9±3.4*

	Dev. Pressure (mmHg)	LVEDP (mmHg)	Systolic Duration (ms)
PBS	92.4±2.3	16.1±0.7	73.6±1.2
IL4	114.1±0.8*	10.1±0.6*	85.6±3.1*

	Diastolic Duration (ms)	Max dP/dt (mmHg/s)	Min dP/dt (mmHg/s)
PBS	97.4±1.4	5170±84	-4815±159
IL4	90.0±6.1	6571±119*	-4480±234

	IRP Average dP/dt (mmHg/s)	Tau (s)	Pressure Time Index (mmHg.s)
PBS	-2159±101	0.0187±0.0004	6.2±0.2
IL4	-2691±183*	0.0285±0.0021*	8.5±0.5*

	Heart Rate (bpm)
PBS	351±3
IL4	345±15

Supplemental Table 3. Catheterization data in the IL-4 treatment study (Day 28 post-MI).
PBS group=injection of PBS; IL-4 group=L-4 treatment; Dev. Pressure=developed pressure; LVEDP=left ventricular end-diastolic pressure; IRP=isovolumic relaxation period; Tau=left ventricular diastolic time constant. n=10 for each group, **P*<0.05 *versus* the PBS group; Student's t-test.